Molecular Cancer Research

AACR

RAS/MEK−Independent Gene Expression Reveals BMP2-Related Malignant Phenotypes in the *Nf1*-Deficient MPNST

Daochun Sun, Ramsi Haddad, Janice M. Kraniak, et al.

Updated version	Access the most recent version of this article at: doi:10.1158/1541-7786.MCR-12-0593
Supplementary Material	Access the most recent supplemental material at: http://mcr.aacrjournals.org/content/suppl/2013/02/19/1541-7786.MCR-12-0593.DC1.html

Cited Articles	This article cites by 57 articles, 22 of which you can access for free at: http://mcr.aacrjournals.org/content/11/6/616.full.html#ref-list-1

E-mail alerts	Sign up to receive free email-alerts related to this article or journal.
Reprints and Subscriptions	To order reprints of this article or to subscribe to the journal, contact the AACR Publications Department at pubs@aacr.org.
Permissions	To request permission to re-use all or part of this article, contact the AACR Publications Department at permissions@aacr.org.

Genomics

RAS/MEK–Independent Gene Expression Reveals BMP2-Related Malignant Phenotypes in the *Nf1*-Deficient MPNST

Daochun Sun[1], Ramsi Haddad[2,3], Janice M. Kraniak[2], Steven D. Horne[1], and Michael A. Tainsky[1,2]

Abstract

Malignant peripheral nerve sheath tumor (MPNST) is a type of soft tissue sarcoma that occurs in carriers of germline mutations in *Nf1* gene as well as sporadically. Neurofibromin, encoded by the *Nf1* gene, functions as a GTPase-activating protein (GAP) whose mutation leads to activation of wt-RAS and mitogen-activated protein kinase (MAPK) signaling in neurofibromatosis type I (NF1) patients' tumors. However, therapeutic targeting of RAS and MAPK have had limited success in this disease. In this study, we modulated NRAS, mitogen-activated protein/extracellular signal–regulated kinase (MEK)1/2, and neurofibromin levels in MPNST cells and determined gene expression changes to evaluate the regulation of signaling pathways in MPNST cells. Gene expression changes due to neurofibromin modulation but independent of NRAS and MEK1/2 regulation in MPNST cells indicated bone morphogenetic protein 2 (*Bmp2*) signaling as a key pathway. The BMP2-SMAD1/5/8 pathway was activated in NF1-associated MPNST cells and inhibition of BMP2 signaling by LDN-193189 or short hairpin RNA (shRNA) to BMP2 decreased the motility and invasion of NF1-associated MPNST cells. The pathway-specific gene changes provide a greater understanding of the complex role of neurofibromin in MPNST pathology and novel targets for drug discovery. *Mol Cancer Res; 11(6); 616–27. ©2013 AACR.*

Introduction

Neurofibromatosis type I (NF1) is a single gene mutation-related disorder with an incidence of 1:3,000 live births. It is well known that the loss-of-function of neurofibromin, a 250 kD Ras GTPase-activating protein (GAP) encoded by *Nf1* gene, leads to hyperactive RAS activity and an increase of mitogen-activated protein kinase (MAPK) pathway signaling in the patients' cells (1, 2). Typical manifestations of an *Nf1* deficiency include benign dermal neurofibromas and plexiform neurofibromas, the latter are located deeply within the peripheral nervous system. In 8% to 13% of NF1 patients, the benign plexiform neurofibromas develop into malignant peripheral nerve sheath tumors (MPNST), usually with a poor prognosis and high mortality (3). Up to 50% of the MPNSTs occur in the context of an *Nf1* genetic disease (4, 5) and the remainder, with a functional wt-*Nf1*, occurs sporadically. NF1-associated MPNST is generally believed to arise from the precursor Schwann cells promoted by the *Nf1* heterozygous microenvironment (6, 7). The success of the primary treatment, surgery, is limited by tumor invasion leading to high relapse rates. RAS–MEK–ERK–targeted therapeutic strategies have met with limited success (8). Discoveries of signal transduction downstream of RAS and of MEK-ERK pathways specific to NF1 disease, or pathways independent of RAS–MEK–ERK could provide new targets for therapeutic purposes (9).

Gene expression studies by microarray have been used to identify the gene signatures associated with MPNSTs. Lee and colleagues first applied the cDNA microarray of 4,608 probes to the comparison of T265 cells, an *Nf1*-deficient cell line, with normal human Schwann cells (HSC) and identified 955 differentially expressed genes (10). Watson and colleagues tested primary human NF1-associated and sporadic MPNST samples by using oligonucleotide microarrays representing 8,100 unique human genes but failed to define a reliable molecular signature to distinguish sporadic and NF1-associated MPNST tissue samples (11). Miller and colleagues compared 8 MPNST cell lines with normal HSCs and identified a 159-gene signature that separated these 2 groups (12). Research from this group then compared primary human samples from several subtypes of neurofibromas and MPNSTs, and the results indicated that the overexpressed gene *Sox9* may serve as a biomarker of survival factor in NF1-related MPNSTs (13). Although these studies have provided enormous data on gene expression changes in MPNSTs, however, the evaluation of drug targets related to

Authors' Affiliations: [1]Center for Molecular Medicine and Genetics; [2]Department of Oncology, Wayne State University School of Medicine, Wayne State University; and [3]Laboratory of Translational Oncogenomics, National Oncogenomics and Molecular Imaging Center, Karmanos Cancer Institute, Detroit, Michigan

Current address for R. Haddad: Department of Biological Sciences, University of Windsor, Room 289-1 Essex Hall, 401 Sunset Avenue, Windsor, ON, N9B-3P4, Canada.

Corresponding Author: Michael A. Tainsky, Wayne State University School of Medicine, 110 E Warren Ave, Detroit, MI 48201. Phone: 313-578-4340; Fax: 313-832-7294; E-mail: tainskym@karmanos.org

American Association for Cancer Research

neurofibromin deficiency or RAS–MEK signaling was not shown.

We designed systematic study of comparisons of the gene expression changes associated with neurofibromin and its major downstream signaling pathways. In brief, genes regulated by NRAS, the predominant RAS protein in MPNST cell lines (1), were identified by siRNA interference, and the mitogen-activated protein/extracellular signal–regulated kinase (MEK)1/2–related genes were characterized by U0126 inhibition in ST88-14 cell line, which is derived from patient with NF1 with mutated neurofibromin (14–16). Neurofibromin-associated gene changes were first characterized by gene profile comparison between ST88-14 and normal HSCs, and further refined by neurofibromin knockdown in STS26T, a sporadic MPNST cell line with the functional, wild-type neurofibromin (17, 18). Using intersection analysis of gene expression profiles under these scenarios, alterations in gene regulation exerted by the neurofibromin-regulated pathways were determined. This strategy enabled us to identify genes related to neurofibromin deficiency but independent of NRAS and MEK1/2 pathways in MPNSTs, with the potential to provide previously unknown mechanisms leading to NF1-related malignancy.

We identified bone morphogenetic protein 2 (BMP2) expression as neurofibromin-regulated but independent of NRAS and MEK1/2. BMP2 belongs to the TGF-β superfamily, and it functions as a morphogen required for the development of lung, heart, and central nerve system. Overexpression of BMP2 has been found in many different types of tumors including gliomas, melanomas, breast cancer, and fibrosarcomas (19–21), and it promotes malignancy-related attributes such as migration and invasion of these tumors (20, 22, 23). We found that inhibition of BMP2 signaling by LDN-193189 or BMP2 short hairpin RNA (shRNA) decreased the motility and invasion of *Nf1*-deficient MPNST cells *in vitro*.

Materials and Methods

Cell culture and chemicals treatment

Human MPNST ST88-14 cell line (a generous gift from T. Glover, University of Michigan, Ann Arbor, MI) and STS26T cell line (a generous gift from D. Scoles, Cedars-Sinai Medical Center, Los Angeles, CA) were maintained in RPMI-1640 medium (Invitrogen) supplemented with 5% FBS (Hyclone Laboratories). T265 cell line (a generous gift from G. De Vries, Hines VA Hospital, Hines, IL) was cultured in Dulbecco's modified Eagle's medium (DMEM; Invitrogen) supplemented with 5% FBS. sNF96.2 and sNF02.2 cell lines were purchased from American Type Culture Collection and cultured in DMEM medium supplemented with 10% FBS. Primary normal HSCs HSC291, HSC361, and HSC338 (generous gifts from Patrick M. Wood, University of Miami Miller School of Medicine, Miami, FL) were cultured in DMEM medium supplemented with 10% FBS, 2 μmol/L forskolin, and 10 nmol/L heregulin. All cell lines were checked periodically for *Myco-*

plasma with Venor GeM Mycoplasma Detection Kit (Sigma-Aldrich). Cultures were propagated for no more than 3 months. To inhibit MAPK activity, 10 μmol/L U0126 (CalBiochem) was applied to the ST88-14 preseeded in 10-cm plate for 18 hours before harvest for mRNA. Parallel cultures for each RNA preparation were used for concurrent controls to show inhibition of the relevant pathway.

siRNA gene knockdown

Human *Nf1* siRNA (si*Nf1*), *NRas* siRNA (si*NRas*), control siRNA, and siRNA Transfection Reagent (Santa Cruz Biotechnology) were used according to the manufacturer's instructions. STS26T cells were plated at 1.5×10^5 cells per 10-cm plate 24 hours before transfection. Four microliter of siRNA (∼30 nmol/L) and 4 μL of siRNA transfection reagent, each diluted in 400 μL of Optimem (Invitrogen), were combined and after a 30-minute incubation added to the 3.2 mL of OptiMem in each plate. The same amount of scrambled control siRNA was used as control. Following 6 hours incubation of cells with the transfection solution, the medium was replaced by growth medium. Cells were harvested 48 hours later. For ST88-14, similar protocols were used for NRAS knockdown. As stated earlier parallel cultures for each RNA preparation were used for concurrent controls to show knockdown of the relevant targets.

Western blots analysis

Cells grown from 30% to 80% confluence were washed with ice-cold PBS, scraped, and then were lysed with radio-immunoprecipitation assay (RIPA) buffer (150 mmol/L NaCl; 1% Triton X-100; 0.5% deoxycholic acid, 0.1% SDS; 50 mmol/L Tris–Cl; pH 8.0) supplemented with 2% protease inhibitor cocktail, 1% phenylmethylsulfonyl-fluoride (PMSF; from stock at 10 mg/mL in methanol), 1 mmol/L Na$_3$VO$_4$, 1 mmol/L Na$_4$P$_2$O$_7$.10H$_2$O, and 1 mmol/L NaF. Secondary antibodies were conjugated to IRdye infrared dyes (Rockland). The protein bands were detected and quantified using the Odyssey infrared imaging system and software (Licor Biosciences).

The antibodies used in these experiments were rabbit polyclonal antineurofibromin (Santa Cruz Biotechnology), goat polyclonal anti-NRAS (Abcam), mouse monoclonal anti-phospho-ERK1/2 and total extracellular signal–regulated kinase (ERK)1/2 (Cell Signaling), rabbit polyclonal anti-ERK1,2 (Cell Signaling), mouse monoclonal anti-α-tubulin (Sigma-Aldrich), rabbit polyclonal anti-SMAD1/5/8 (Cell signaling), and mouse polyclonal anti-total SMAD1/5/8 (Abcam). Neurofibromin were run on 8%, ERK1/2 and SMAD1/5/8 on 10%, and NRAS on 15% SDS-PAGE, respectively. Eighty microgram of protein lysate was loaded in each well, and nitrocellulose transfer membrane (Protran, Whatmann GmbH) was used for protein transfer.

RNA isolation and microarray analysis

Total RNA was extracted from the cells using RNeasy Mini Kit (Qiagen) with genomic DNA removal by RNase-Free DNase Set (Qiagen). RNA integrity was determined by

an Agilent Bioanalyzer 2100. Labeled targets were synthesized from the purified RNA using linear amplification and indirect labeling by incorporation of aminoallyl-labeled nucleotide with the TargetAmp one-round aminoallyl-aRNA amplification kit 101 (Epicentre Technologies), which was subsequently modified by the covalent addition of Alexa dye (Epicentre Technologies).

Agilent whole human genome 4×44 K 2 color microarray platform was used to characterize the gene profile, which covered more than 41,000 genes and transcripts of human genome. Three independent replicates of each RNA preparations were isolated on different occasions to account for biologic variation. Probe intensities were normalized by Lowess normalization and differential gene expression was determined using the "limma" package in Bioconductor in an R environment. Differentially expressed genes for pathway analysis were determined by adjusted P value less than 0.01 and fold change (upregulated or downregulated) more than 1.5 for most of the comparisons. In the comparison between ST88-14 and normal HSCs, many differential expressed genes were identified. We increased the stringency for this comparison by lifting the adjusted P value threshold to less than 1×10^{-6}, and final numbers of differentially expressed genes are shown in Supplementary Table S1. Around 60 genes were chosen to verify the microarray results by quantitative PCR (qPCR) and approximately 97% were confirmed. The verified list of genes and primers are provided in Supplementary Table S5. The raw data of the microarray were submitted to Gene Expression Omnibus as GSE39764.

Gene Ontology and pathway analysis

Ingenuity Pathway Analysis (IPA) software (Ingenuity System, http://www.ingenuity.com) and Genomatix software suite (http://www.genomatix.de/) were used in the gene function enrichment and pathway analysis. Generally, gene official names with fold-change data from different datasets were used as input. Each software package can generate the significant biologic terms or pathways based on the classic knowledge and latest literatures. All the analyses were conducted following the manufacture instructions and default settings.

Quantitative real-time PCR using SYBR green I

Three batches of independent total RNA from the same preparations used for microarray were reverse transcribed by SuperScript First-Strand Synthesis System (Invitrogen). ABI 7500 Sequence Detection System was used to determine the relative quantity of a specific gene in the cDNA template. Primer sequences for validation are shown in Supplementary Table S5.

Lentivirus shRNA-mediated stable *NRas* knockdown and inducible oncogenic RAS expression system

MPNST cell lines targeted for stable gene knockdown or using a nonsilencing sequence were constructed by lentivirus based shRNA technology. The lentivirus vector containing shRNAs targeting NRAS and scrambled sequence were packaged using the Trans-Lentiviral Packaging System

(TLP4615, Open Biosystem, Thermo) in 293T cells. The virus particles were harvested and titered according to the manufacturer's protocol. The ST88-14 cells were incubated with viral particles for 4 hours and selected by 0.5 μg/mL puromycin for 5 days. Drug-selected pooled cells were confirmed to be virally infected by fluorescence microscopy for GFP expression and further verified by qPCR.

Tet-off (BD Biosciences) cell line conditionally expressing the oncogenic form of RAS-G12V was established using the parent Schwann cell line STS26T. The procedure is described in a previous study [Kraniak and colleagues 18].

Scratch recovery cell migration assay

Cells were seeded at 1×10^{6} cells per well in 6-well plates and preincubated with LDN-193189 at the same concentrations used in the scratch experiment overnight. The scratch was made on 100% confluent cell monolayer by a plastic tip. To quantify the cell migration images, we used T265 and ST88-14 infected by the GFP-expressed lentivirus to create T265*Non*KD and ST88*Non*KD cell lines. T265*Non*KD cells were cultured at 0.1% or 5% FBS with 0, 0.001, 0.01, and 0.1 μmol/L LDN-193189. Because ST88*Non*KD survived poorly with 0.1% FBS, 1% FBS was used in those experiments. ST88*Non*KD cells were cultured at 1% and 5% FBS with same LDN-193189 concentration series. Cell migration was monitored after 24 hours of cell culture by Olympus IX71 fluorescent microscope, and the area of the scratched region (the dark gap) was quantified in terms of the number of pixels by slidebook 4.2 (Olympus). The more cells that migrated to the area, the less was number of pixels in the dark gap. This assay was repeated at least 3 independent occasions under each of the conditions.

Matrigel invasion assay

BD BioCoat Growth Factor Reduced Matrigel invasion Chamber was used to access the invasion ability of the ST88-14 and T265. Briefly, 2.5×10^{4} cells were added to the upper chamber coated by Matrigel without serum but with the BMP2 and/or LDN-193189. Cells were stimulated by 200 ng/mL BMP2 for 24 hours in the chamber before evaluation. Cells with LDN-193189 were pretreated with 0.1 μmol/L LDN-193189 overnight before seeding to the chambers, and the medium was changed to fresh 0.1 μmol/L LDN-193189 with/without BMP2 200 ng/mL for 24 hours for evaluation. Five percent FBS was used as attractant in the lower chamber. After 24 hours, the cells remaining in the chamber were removed by the cotton swab and invaded cells present on the other side of the bottom of chamber were fixed and stained by Diff-Quick Stain (Biochemical Science, Inc.). The invaded cells were counted under a microscope and all experiments were repeated 3 times following the manufacturer's instructions.

Statistics analysis

Experiments were subject to at least 3 independent replicates. For qPCR and scratch assay results, paired t test was used to determine the significant differences at 95% or 99% confidence interval.

Results

Pathway intervention and intersection analysis scheme in MPNST cell lines

To characterize neurofibromin-dependent gene expression, we applied pathway-specific interventions. Using chemical and genetic pathway interference in ST88-14 cells, we identified gene expression profiles related to MEK1/2 and NRAS. The comparison between ST88-14 and normal HSCs was used to capture the gene space deregulated during tumorigenesis after loss of the *Nf1* gene in ST88-14 cells. Gene expression changes specific to an *Nf1* deficiency were determined by siRNA interference to *Nf1* gene in STS26T, a sporadic MPNST cell line with functional neurofibromin. Using Agilent whole human genome 4×44 K 2 color microarrays, we investigated neurofibromin, NRAS, and MEK1/2-related gene expression profiles.

The differentially expressed gene changes were defined as the following datasets (DS):

DS-1) siRNA-targeted knockdown of human *Nf1* (vs. a scrambled control siRNA) in STS26T was conducted to distinguish the gene changes specific to an *Nf1* deficiency.

DS-2) siRNA-targeted knockdown of human *NRas* (vs. a scrambled control siRNA) in ST88-14 was conducted to identify *NRas* knockdown-associated gene changes.

DS-3) Administration of the MEK1/2 inhibitor, U0126 (vs. DMSO control) to ST88-14 to identify MEK1/2 pathway–influenced genes.

DS-4) Comparison of ST88-14 versus normal HSC to identify gene expression changes associated with an *Nf1*-related tumorigenesis.

The number of differently expressed genes for each comparison are summarized in Supplementary Table S1 and the gene lists of all the datasets are presented in Supplementary Table S2.

In ST88-14 cells, the si*NRas* decreased expression of NRAS at the protein level by approximately 60% and decreased phosphorylated ERK1/2 by approximately 50%, confirming that hyperactive NRAS is a strong upstream signal activating the MEK1/2–ERK1/2 pathway in ST88-14 cells (Supplementary Fig. S1A). U0126, an inhibitor of MEK1/2 in NF1-associated MPNST cells (1, 18), reduced the level of phosphorylated ERK1/2 by approximately 90% after 18 hours treatment at 10 μmol/L (Supplementary Fig. S1B). In the sporadic MPNST cell line STS26T, si*Nf1* the knockdown efficiency after 48 hours was approximately 90% at the protein level compared with the scrambled control siRNA treated (Supplementary Fig. S1C). Phosphorylated ERK1/2 increased by 1.6-fold in si*Nf1*-treated STS26T cells (Supplementary Fig. S1C), and the transcription factor activity of activator protein 1 (AP1) increased as observed in our previous study (18), indicating that the neurofibromin–NRAS–MEK1/2 axis was functional in STS26T cells.

The differentially expressed gene lists from each comparison provided the basis for the intersection analysis of the gene expression profiles. The overlapping genes were then classified into cell signaling axes based on their patterns of change as defined in Table 1. For example, given that MEK1/2 is downstream of NRAS, if a gene is upregulated when NRAS is inhibited, and is also upregulated when MEK1/2 is inhibited, the regulation of this gene was considered to be under the control of NRAS–MEK1/2 axis meaning that the suppressed NRAS may upregulate that gene through the decreased activity of MEK1/2. With such reasoning based on the biologic pathways, we associated the overlapping genes to the specific signaling axes, and defined the neurofibromin-related but NRAS and MEK1/2 independent genes.
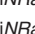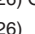
Intersection analysis reveals the pathway related potential drug targets in ST88-14 cells

As we expected, in ST88-14 cell line, when comparing the lists of genes from any 2 of 3 experimental conditions (ST88-14 vs. HSC, si*NRas* vs. control, and U0126 vs. DMSO), we found a substantial number of shared genes (Table 1). This showed that our methods of inhibition, si*NRas* and U0126, were functionally consistent. When comparing ST88-14 and HSC, the differentially expressed genes were large probably due to the process of tumorigenesis along with those regulated by the loss of wild-type neurofibromin. We used *Nf1* knockdown in STS26T cells to delineate those changes in gene expression specific to the neurofibromin deficiency rather than those simply associated with tumorigenesis.

The loss-of-function of neurofibromin and hyperactive NRAS have been characterized in ST88-14 cells (1, 18). To identify specific targets of neurofibromin–NRAS axis (DS-5), we defined 2 patterns of gene expression change in the comparisons of ST88-14 versus HSC (DS-4) and si*NRas* versus scrambled control (DS-2): (i) gene expression upregulated in DS-4 but downregulated in DS-2, or (ii) downregulated in DS-4 but upregul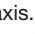ated in DS-2 (Table 1; DS-5 in Supplementary Table S2). Gene set enrichment analysis (GSEA) program by Genomatix Pathway System (GePS; ref. 24) revealed that Gene Ontology (GO) terms in biologic process such as "positive regulation of heart contraction" (GO: 0045823), including genes *Adm* and *Tpm1* and "cellular component morphogenesis" (GO: 0032989), including genes *Adm*, *Met*, *Ptprz1*, *Tpm1*, and *Smad3* were significantly enriched (Supplementary Table S3). Another interesting gene revealed in these patterns was *Rgs16*, which can activate the GTPase of G-protein α unit so as to inhibit the signal transduction through G-protein coupled receptors. RGS16 expression in ST88-14 decreased by 5.6-fold compared with the normal Schwann cells and increased by about 2-fold in the si*NRas* treated compared with the scramble control siRNA treated. This pattern suggested *Rgs16* expression was regulated by neurofibromin–NRAS and negatively associated with the increased NRAS activity. Considering the complex signaling downstream of G-protein subunits including ERK1/2, phosphoinositide 3-kinase (PI3K), and adenylate cyclases, the downregulation of *Rgs16* by increased NRAS could serve as another strong enhancer in MPNST tumorigenesis. The loss of *Rgs16* has been reported in some breast cancers, which facilitated the PI3K signaling (25).

Table 1. Definition of dataset and signaling axis association

Dataset	Intersection operation	Pattern definition	Gene	Signaling axis
DS-5	DS-4 ∩ DS-2	(↑ in ST88 ↓ in siNRas) OR (↓ in ST88 ↑ in siNRas)	22	**Neurofibromin-NRAS** in ST88-14
DS-6	DS-4 ∩ DS-3	(↑ in ST88 ↓ in U0126) OR (↓ in ST88 ↑ in U0126)	208	**Neurofibromin-MEK1/2** in ST88-14
DS-7	DS-2 ∩ DS-3	(↑ in siNRas ↑ in U0126) OR (↓ in siNRas ↓ in U0126)	20	**NRAS-MEK1/2** in ST88-14
DS-8	DS-4 ∩ DS-2 ∩ DS-3	(↑ in ST88 ↓ in siNRas ↓ in U0126) OR (↓ in ST88 ↑ in siNRas ↑ in U0126)	5	**Neurofibromin-NRAS-MEK1/2** in ST88-14
DS-9	DS-4 \ (DS-2 U DS-3)	(↑ OR ↓ in ST88) NOT IN (siNRas and U0126)	2697	**NRAS-MEK1/2 independent** in ST88-14
DS-10	DS-1 ∩ DS-9	(↑ in siNF1) AND [(↑ in ST88) NOT IN (siNRas AND U0126)] OR (↓ in siNF1) AND [(↓ in ST88) NOT IN (siNRas AND U0126)]	73 142	**Neurofibromin related NRAS-MEK1/2 independent** in MPNSTs

NOTE: The patterns of gene expression change in dataset comparison were defined to associate the genes to the specific signaling axis. ↑, increase; ↓, decrease; ∩, intersection operation; U, union operation; \, relative complement operation; AND, OR, NOT IN: logic operation.

Gene expression that increased in ST88-14 compared with HSC in DS-4 and decreased in the U0126-treated cells compared with DMSO treated in DS-3, or alternately decreased in DS-4 but increased DS-3, could be the regulatory targets of neurofibromin–MEK1/2 axis (Table 1; DS-6 in Supplementary Table S2). GSEA indicated that ontology terms such as "cell cycle" (GO: 0007049; $P = 7.65e-8$), "cell-cycle arrest" (GO: 0007050; $P = 3.49e-7$) and "regulation of serine/threonine kinase activity" (GO: 0071900; $P = 3.48e-4$) were among the most significant terms. These biologic process terms were consistent with the ERK1/2 suppression related cell-cycle arrest (26) and inhibitory effects of U0126 on MEK1/2 (1), indicating that deregulation of these processes occurred after defects of neurofibromin–MEK1/2 in MPNSTs. *Sox9*, which was present in DS-6, has been reported as a biomarker in MPNSTs because of its overexpression in NF1-related malignancies and its role in the tumor survival (13). Our data confirmed that the *Sox9* expression was higher in ST88-14 compared with HSC and that *Sox9* expression can be downregulated by U0126. In addition, *Sox9* expression did not change in the si*NRas*-treated samples, which indicated a possible mechanism in which *Sox9* expression was regulated through neurofibromin–MEK1/2 but not by NRAS in ST88-14 cells.

In DS-6, we observed *Edn1* (endothelin 1) to be strongly inhibited by U0126, indicating that the MEK1/2 signaling was prominent in its regulation. Results from Ingenuity Pathway Analysis (IPA) identified that among the genes previously reported to be regulated by EDN1, mRNA expression of 8 genes was positively associated with mRNA level of *Edn1* in DS-6, consistent with literature supported trend of change, including *Apln*, *Cdc25a*, *Egfr*, *Errfi1*, *Fst*, *Il8*, *Mmp9*, and *Ptger4* (Supplementary Table S4). EDN1 is a secreted protein with multiple physiologic effects on cellular development, differentiation, vasoconstriction, and mitogenesis (27) and it may be an important effector under the regulation of neurofibromin–MEK1/2 axis during development and tumorigenesis.

Comparing DS-2 (si*NRas* vs. control) and DS-3 (U0126 vs. DMSO), genes both upregulated or both downregulated in the 2 different datasets were identified as under the control of NRAS–MEK1/2 axis (Table 1; DS-7 in Supplementary Table S2). Ecto-5′-nucleotidase (NT5E) that converts AMP to adenosine was downregulated in both datasets, and Sunaga and colleagues reported that NT5E was downregulated in non–small cell lung carcinoma (NSCLC) lines with KRAS knockdown (28). NT5E has also been associated with cell cycle and apoptosis in breast cancer, arterial calcifications, and immunodeficiency diseases (29–31). Our study indicated its expression was positively controlled by NRAS–MEK1/2 axis in ST88-14 cells.

Identification of neurofibromin-related gene expression changes independent of NRAS and MEK1/2 pathways in MPNST cells

For the 3 comparative scenarios involving ST88-14 cells (Fig. 1), removal from DS-4 of the genes that overlapped with DS-2 and with DS-3 enabled us to identify those genes that were independent of the NRAS and MEK1/2 pathways, namely DS-9 (Fig. 1; Table 1; and DS-9 in Supplementary Table S2). We then created a dataset of genes directly associated with *Nf1*-inhibition using siRNA as compared with scrambled control siRNA in STS26T cells (DS-1). By overlapping DS-9 with DS-1, we identified 142 unique genes that were downregulated and 73 unique genes that were upregulated in both DS-1 and DS-9 (Supplementary

Figure 1. Scheme of intersection analysis of gene profiles. The intersection analysis of gene expression profiles under different senarios is indicated by Venn diagram. The comparison scheme to identify expression changes associated with neurofibromin but independent of NRAS and MEK1/2 pathways is indicated. SC: scrambled siRNA-treated samples.
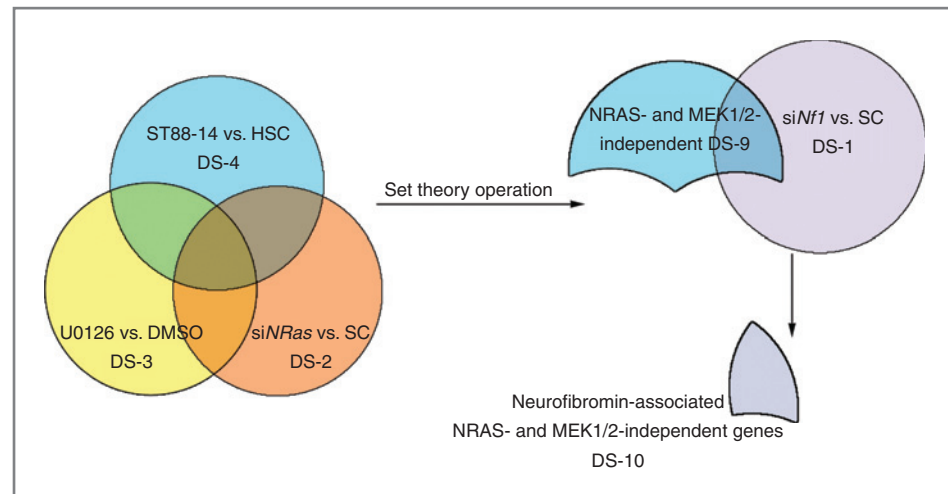
Table S2 and Supplementary Fig. S1). We considered these genes, DS-10, to be under the regulation of neurofibromin, but independent of the NRAS and MEK1/2 pathway.

For the upregulated changes, GSEA revealed that GO term "RAS GTPase binding" (GO: 0017016; $P = 4.70e-4$) including *Dock4*, *Myo5b*, *Srgap1*, and *Als2* indicated multiple regulatory mechanisms of activated RAS after loss-of-function of *Nf1*. The GO term "SMAD signal transduction" (GO: 0060395; $P = 1.16e-3$) including *Hipk2* and *Bmp2* was significant (Supplementary Table S3). Interestingly, the significance of "signaling by BMP2" was reported by pathway analysis of GePS as well, which drew our attention to the aberrant expression of *Bmp2* in *Nf1*-deficient MPNSTs.

Bmp2 overexpression is independent of NRAS and MEK1/2 in MPNSTs but related to neurofibromin function

As members of TGF-β superfamily, BMPs play various roles in morphogenesis and homeostasis in many tissue types during the development. Recent studies have indicated a role for BMPs in molecular processes associated with different human cancers (32). Interestingly, we also found *Bmp2* as one of 2,827 differentially expressed transcripts in Miller's microarray data (13) on NF1-associated tissue samples, and based on graphical analysis of that data, we found that there was a positive association between *Bmp2* expression and the degree of malignancy in clinical samples of NF1-associated tumors (Supplementary Fig. S2).

We verified differential gene expression of *Bmp2* by qPCR under the experimental conditions analyzed for gene profiles (Fig. 2A). Consistent with the microarray data, *Bmp2* mRNA was overexpressed in ST88-14 compared with the normal HSC and there was no significant difference for *Bmp2* mRNA in ST88-14 cells treated with U0126 or si*NRas* compared with their controls. We used 3 different si*Nf1* oligos to verify the association between neurofibromin knockdown and *Bmp2* expression in STS26T cells. All 3 of the oligos significantly inhibited the neurofibromin and increased the *Bmp2* mRNA expression (Fig. 2B). We next used an inducible oncogenic RAS expression system in the

STS26T cell line to mimic the loss function of GTPase-activating domain of neurofibromin (18), and thereby studied the RAS dependence of *Bmp2* expression in MPNST cells. Forty-eight hours after removal of doxycycline from the cultural media, oncogenic RAS was induced as indicated by increased ERK1/2 phosphorylation (Supplementary Fig. S3). However, *Bmp2* expression was not significantly altered by increased RAS activity in this cell model (Fig. 2C), indicating that *Bmp2* mRNA changes were indeed dependent on neurofibromin but independent of the RAS-related pathway activity.

BMP2 regulation of Smad1/5/8 activity is independent of NRAS in MPNST cells

In the canonical signaling, BMP2 exerts its function by binding to specific type I and II receptors to form a complex with serine–threonine kinase activity, which subsequently results in phosphorylatation of SMAD1/5/8. Phosphorylated SMAD1/5/8 proteins bind to SMAD4 and translocate to the nucleus to regulate gene expression (33). However, the roles of BMP2 in tumorigenesis are diverse including the epithelial-to-mesenchymal transition, metastasis, and angiogenesis (32). We found that SMAD1/5/8 phosphorylation was increased in 3 independent NF1-deficient MPNST cell lines, ST88-14, T265, and sNF96.2, compared with normal HSCs (Fig. 3A). The BMP2-SMAD1/5/8 pathway activity in ST88-14 was further evaluated by BMP2 stimulation after serum starvation. Treating these cells with 100 ng/mL BMP2 stimulated the phosphorylation of SMAD1/5/8 in 15 minutes after overnight serum starvation, with limited additional phosphorylation after BMP2 treatment at 200 ng/mL (Fig. 3B). Because BMP2 was overexpressed in MPNST cells, we suspected that the overexpressed BMP2 could promote SMAD1/5/8 activity. Further analysis of this pathway in these cells revealed that si*Bmp2* treatment of ST88-14 cells resulted in a approximately 60% reduction in *Bmp2* mRNA expression as determined by qPCR (Fig. 3C) and inhibition of phosphorylation of SMAD1/5/8 (Fig. 3D).
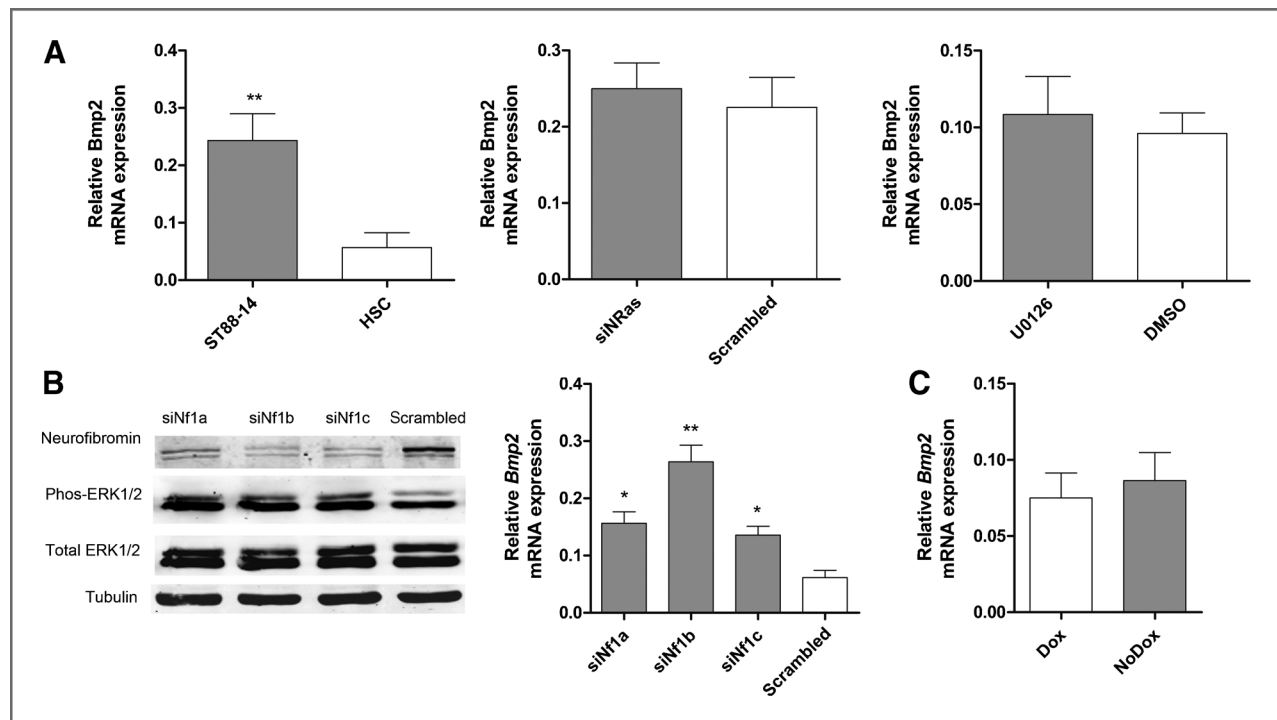
Figure 2. Verification of Bmp2 expression by qPCR in MPNST cell lines at various conditions. A, the expression of Bmp2 mRNA under the conditions for gene profiling in ST88-14 cells was determined. Data are presented as the mean ± SD of 3 independent experiments, paired t test, $n = 3$; **, $P < 0.01$. B, neurofibromin was inhibited by 3 different siNf1 oligos in STS26T cells. Phos-ERK1/2 increased in 24 hours after Nf1 knockdown. Tubulin served as loading control in Western blotting. The figure represents 1 of 3 independent Western blot analyses. The bar graph represents the increased Bmp2 expression after Nf1 knockdown as mean ± SD of 3 independent experiments, paired t test; $n = 3$; *, $P < 0.05$; **, $P < 0.01$. C, the Bmp2 mRNA expression in STS26T cells without doxycycline (NoDox) and with doxycycline (Dox). Oncogenic RAS was induced by removing doxycycline from media. The data are shown as mean ± SD of 3 independent experiments.

We found negative regulation of SMAD1/5/8 signaling due to NRAS suppression using si*NRas* knockdown in ST88-14 cells resulting in approximately 40% reduction of SMAD1/5/8 phosphorylation. However, when si*Bmp2* was transfected into ST88-14 cells, the phosphorylation of SMAD1/5/8 was inhibited by approximately 80%, substantially greater than that from the *NRas* knockdown alone (Fig. 3D). A combination of siNRas and siBmp2 failed to inhibit phosphorylation of SMAD1/5/8 beyond that of siBmp2 alone, indicating that the SMAD1/5/8 phosphorylation was mainly regulated by BMP2 signaling. A similar conclusion was supported by results observed in NRas stable knockdown cell line (ST88*NRas*KD) and nonsilencing control cell line (ST88*Non*KD; Fig. 3E). As shown, the SMAD1/5/8 phosphorylation decreased in ST88*NRas*KD compared with ST88*Non*KD, and the siBMP2 can further decrease the SMAD1/5/8 phosphorylation in the ST88*NRas*KD cell line, which showed the dominant role of BMP2 signaling to control SMAD1/5/8 phosphorylation. Our data are consistent with a recent report indicating that suppression of RAS activity by salirasib, a S-trans, trans-farnesylthiosalicylic acid (FTS), inhibited the expression of *Bmp4*, and thereafter perturbed BMP4-related SMAD signaling in MPNST cell lines (34). However, we did not find decreased *Bmp4* expression after inhibition of *NRas* by siRNA in our array data. Together, these data indicated that although both

NRAS and BMP2 can control downstream SMADs, BMP2 exerted greater and independent influence on the phosphorylation of SMAD1/5/8 compared with NRAS.

Blocking BMP2 signaling by LDN-193189 and shRNA knockdown impairs the migration and invasion of MPNSTs *in vitro*

Late-stage MPNST frequently metastasizes to the lungs, lymph nodes, and liver, processes that require cellular migration and invasion into tissues (35). Because BMP2 expression increases in the NF1-related malignant tumors (ref. 13; see Supplementary Fig. S2), BMP2 may affect malignancy via enhancement of cell migration and invasion (22, 36). Therefore, we functionally assessed whether these malignant properties were BMP2-regulated in MPNST cell lines. We used LDN-193189, a potent inhibitor of BMP2 binding to its preferred type I receptors, ALK2, ALK3, and ALK6 (37), and thereby BMP2-SMAD1/5/8 signaling. We evaluated the inhibition efficacy of LDN-193189 at different concentrations and the time dependency in MPNST cells to optimize the drug application. We found that treatment to MPNST cells with 0.01 μmol/L LDN-193189 for 1.5 hours can inhibit phosphorylation of SMAD1/5/8 nearly completely (Supplementary Fig. S4) and this concentration is lower than that reported to have significant side effects (37). Next, we tested the migration of
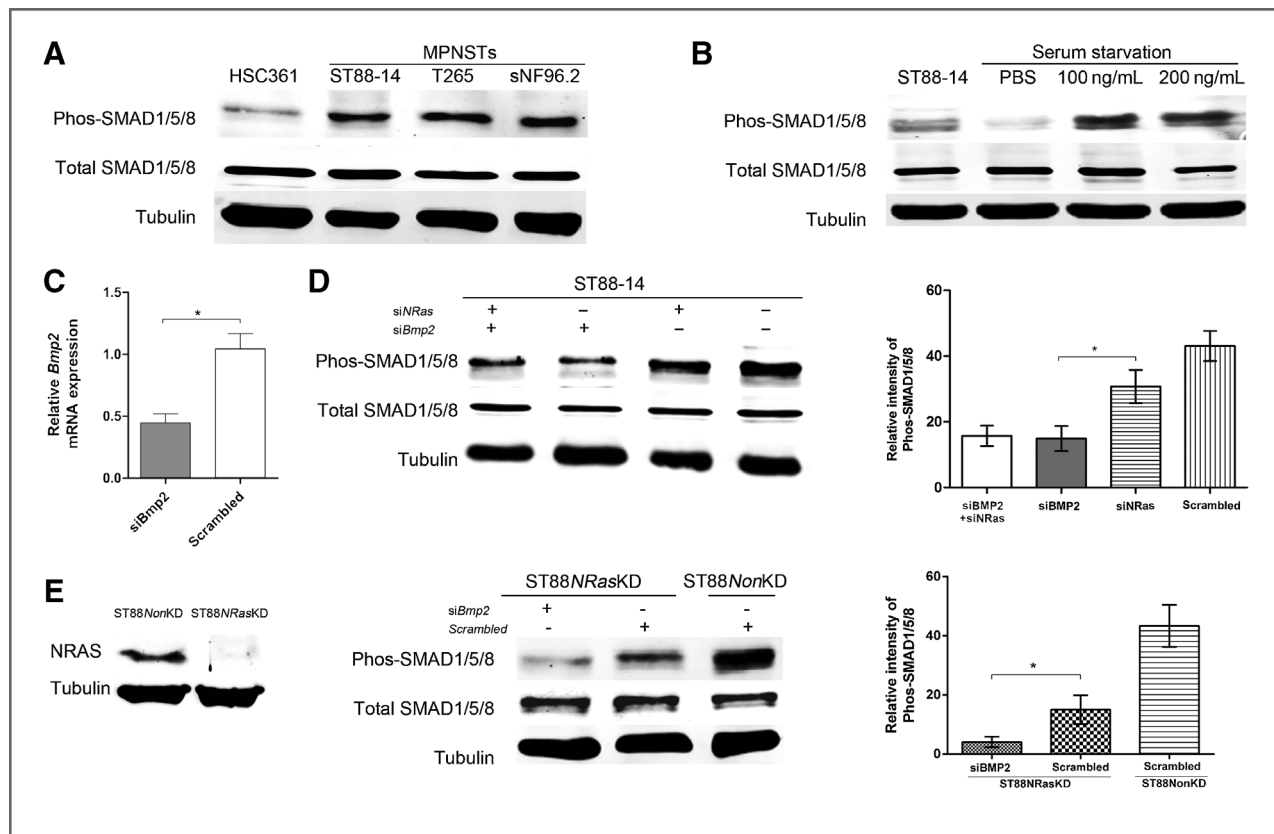
Figure 3. Status of phosphorylated SMAD1/5/8 in MPNST cell lines. A, Western blot analyses indicate higher phosphorylation of SMAD1/5/8 in the MPNST cell lines compared with the normal HSC (HSC361). B, BMP2 stimulation of 15 minutes was applied to ST88-14 after overnight serum starvation (SS). Of note, 100 ng/mL BMP2 increased the phosphorylated SMAD1/5/8 about 2-fold compared with PBS-treated control. Of note, 200 ng/mL had limited effects to further increase the phosphorylation. C, siBmp2 significantly decreased the Bmp2 mRNA expression in ST88-14 cells in qPCR. Data are presented as mean ± SD of 3 independent experiments, paired *t* test; n = 3; *, *P* < 0.05. D, both siNRas and siBmp2 decreased the phosphorylation of SMAD1/5/8, however, siBmp2 significantly inhibited SMAD1/5/8 phosphorylation than siNRas alone. E, NRas protein is hardly detectable in the stable NRas knockdown cell line, ST88NRasKD, compared with the control cell line, ST88NonKD. Even the phosphorylation of SMAD1/5/8 in ST88NRasKD decreased compared with ST88NonKD, 48 hours after siBmp2 treatment, the phosphorylated SMAD1/5/8 decreased significantly compared with the scrambled siRNA-treated ST88NRasKD cells. The densitometry data of Western blot analyses is normalized to the intensity of total SMAD1/5/8 and tubulin, respectively. Data are presented as mean ± SD of 3 independent experiments, paired *t* test; *n* = 3; *, *P* < 0.05.

MPNSTs with various concentrations LDN-193189, and quantified ability of cells to migrate into a scratched gap in the cell monolayer. We quantified the cell migration images of 2 MPNST cell lines, T265NonKD and ST88NonKD, previously infected by lentivirus with nonsilencing shRNA expressing a GFP. Using 0.1% and 5% FBS in T265NonKD, we measured the area of the gap with different LDN-193189 concentrations by determining the number of pixels in the gap (Fig. 4A). There was significant decrease in the motility of cells into gap area using 0.01 μmol/L LDN-193189 24 hours after the scratch. To be assured that the growth rates were not influencing cell migration in the scratch assay, we determined the growth rate of the cell line T265NonKD with different concentrations of LDN-193189 and FBS and found there was no significant growth retardation resulting from the LDN-193189 application at this concentration (Supplementary Fig. S5). A similar inhibitory effect of LDN-193189 on cell migration was observed in ST88NonKD cells (Supplementary Fig. S7). On the

contrary, we did not find *Bmp2* overexpression in STS26T, a sporadic MPNST cell line with wild-type neurofibromin, and LDN-193189 treatment of GFP expressed STS26T cells, STS26TNonKD, did not inhibit the migration of this cell line (Fig. 4B).

To further confirm the specificity of BMP2-related migration, we constructed the stable *Bmp2* knockdown line, ST88Bmp2KD, and compared its migration with the nonsilencing control, ST88NonKD (Fig. 4D). We used 1% FBS because of the poor tolerance of ST88-14 cells to low FBS. *Bmp2* knockdown led to significant decrease in migration of these 2 cell lines at 1% or 5% FBS concentrations at 24 hour after the scratch (Fig. 4C), with no significant difference in the growth rate (Supplementary Fig. S6), thus again excluding influences resulting from cell growth in scratch assay.

The effect of BMP2 on the invasive properties of MPNST cells was measured by low growth factor Matrigel invasion assays. Matrigel was placed on the bottom of the membrane in the upper chamber, and the cells that digested the Matrigel
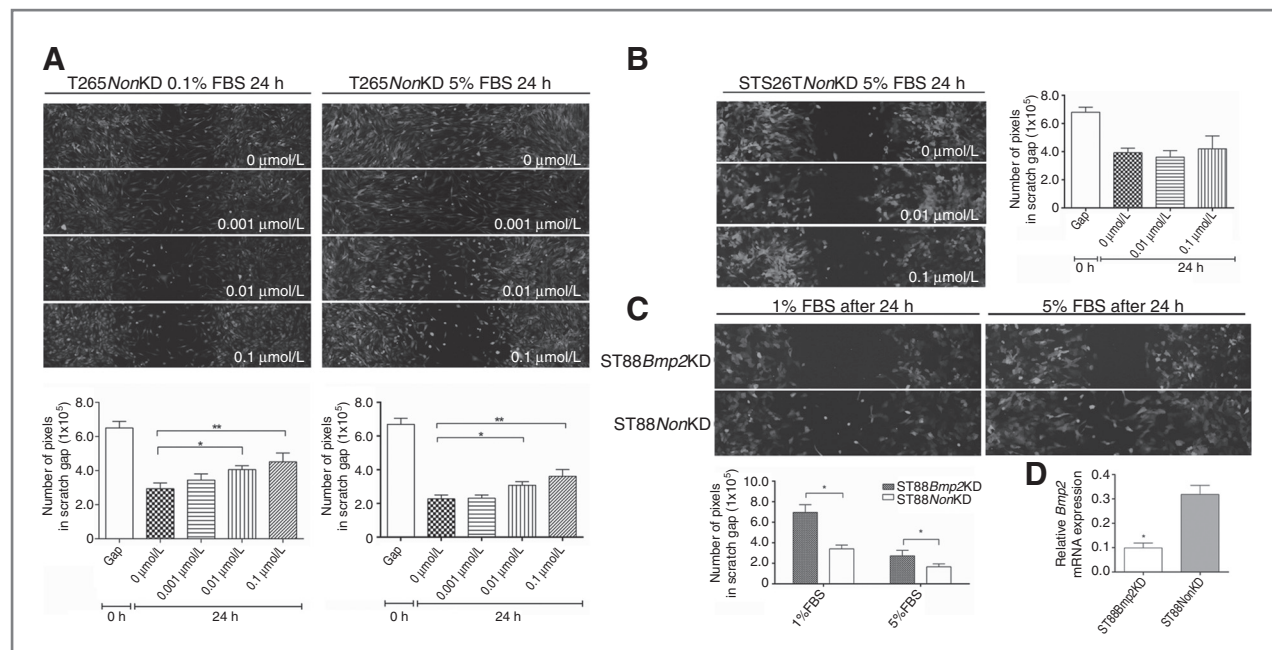
Figure 4. Inhibitory effects on migration of MPNST cells by blocking BMP2 signaling. A, scratch assay indicated that the LDN-193189 treatment inhibited T265NonKD migration at 0.1% FBS and 5% FBS. Images were captured under the fluorescent microscope at 24 hours after scratches representing 1 of 3 replicates. The number of pixels in the gap (the dark area) was quantified and data are presented in bar graph as mean ± SD, paired t test; $n = 3$; *, $P < 0.05$; **, $P < 0.01$. B, different concentrations of LDN-193189 did not influence the migration of STS26TNonKD cells at 24 hours after scratch with 5% FBS culture medium. C, Bmp2 stable knockdown inhibited the migration of ST88-14 cell line significantly. ST88Bmp2KD and ST88NonKD at 1% FBS and 5% FBS were applied to scratch assay. Images were captured under the fluorescent microscope at 24 hours after scratches representing 1 of 3 replicates. The pixels in the gap (the dark area) were quantified and presents as mean ± SD in the bar graph, paired t test; $n = 3$; *, $P < 0.05$. D, qPCR indicated that the endogenous Bmp2 expression were significantly inhibited by the shRNA lentivirus in ST88-14, paired t test; $n = 3$; *, $P < 0.05$.

and invaded through the 8-μm pores were counted on the other side of the membrane. Medium with 5% FBS in the well of each 24-well plate was used as the attractant, and BMP2 and/or LDN-193189 were added into the serum-free medium in the upper chamber with the cells. After 24 hours, cells on the other side of membrane were stained by Quick-Diff and counted using microscopy. We used 200 ng/mL BMP2 and 0.1 μmol/L LDN-193189 to ensure the effective concentration for 24 hours. The invasion of MPNST cells was significantly increased by 200 ng/mL BMP2 stimulation, and the addition of LDN-193189 completely blocked the effect induced by BMP2 in MPNST cell invasion (Fig. 5). *Bmp2* stable knockdown cells, ST88*Bmp2*KD, and T265*Bmp2*KD, also had reduced invasive properties compared with ST88*Non*KD and T265*Non*KD, respectively (Supplementary Fig. S8). Therefore, abrogation of BMP2 signaling in NF1-deficient MPNST cells impaired the cellular migration and invasive properties of these cells, which suggests that BMP2 signaling could promote these malignant properties of MPNSTs *in vivo*. Collectively, these data indicate that the migration and invasiveness of MPNST, as the malignancy-related properties, could be reduced by using BMP2 as a molecular therapeutic target.

Discussion

The RAS-GAP domain of neurofibromin is the most well-studied functional domain in this large, 250 kD protein.

However, the malignant phenotypes of neurofibromin-deficient MPNST cells cannot be totally rescued by the GAP domain reconstitution alone (38, 39). Furthermore, RAS-targeted therapeutic approaches, such as S-trans, trans-farnesylthiosalicylic acid, have provided limited efficacy in clinical studies of NF1 (8, 40). This implies that understanding the full complexity of neurofibromin function in MPNSTs requires insights into all *Nf1*-associated biologic processes not only those dependent on RAS–MEK–ERK signaling but also those independent of that pathway. In this study, we conducted pathway-specific interventions to the MPNST cell lines using genetic and chemical methods. Comparative analysis of gene expression changes across these treatments enabled us to classify those changes that were specific to the NRAS and MEK1/2 pathways, and further to discover novel neurofibromin-related changes in MPNST cell lines independent of those pathways. These genes have potential as drug targets based on their specific mechanisms of regulation.

This is the first study that associates gene expression changes to Ras/MEK1/2–independent pathways resulting from NF1 deficiency in MPNST cell lines. The identification of novel neurofibromin-related gene expression changes that are independent of the NRAS and MEK1/2 pathways was the major goal of this study. We summarized gene changes independent of NRAS and MEK1/2 in ST88-14 as DS-9, and DS-9 was further refined with neurofibromin

Figure 5. BMP2 signaling influenced the invasiveness of ST88-14 and T265 cells. With the 0.1 μmol/L LDN-193189 in medium of the upper chamber for 24 hours, the number of cells invaded through the Matrigel significantly decreased in both ST88-14 and T265 cells comparing with the respective controls without treatments. Of note, 200 ng/mL BMP2 in media of the upper chamber for 24 hours promoted the invasion of 2 cell lines comparing with controls, and the BMP2-related effects were blocked by LDN-193189. Data are presented as mean ± SD of 3 independent replicates in the bar graph, paired *t* test; $n = 3$; *, $P < 0.05$.
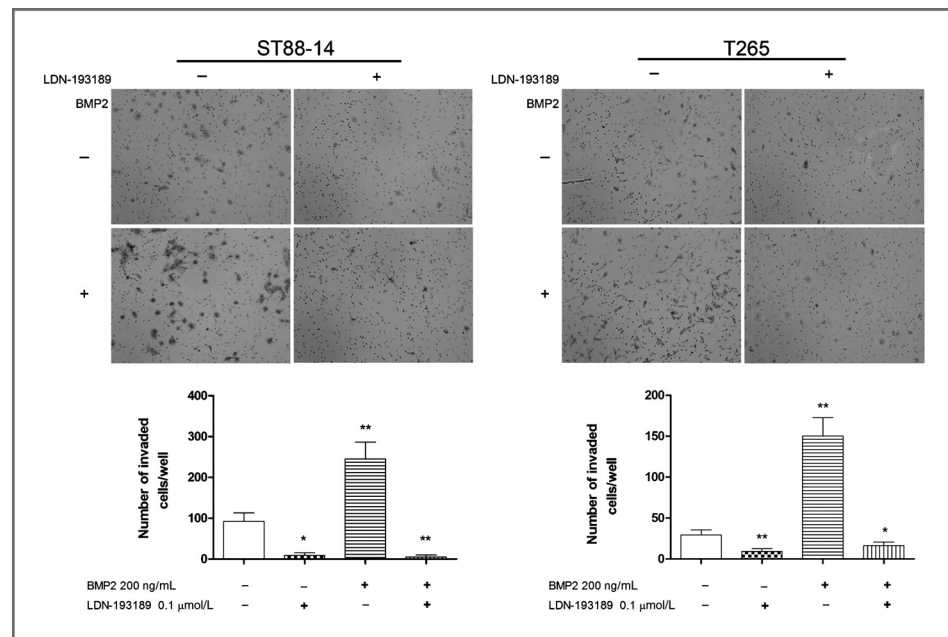
knockdown in STS26T cells to create DS-10 resulting in the identification of neurofibromin-related but NRAS- and MEK1/2-independent changes in multiple *Nf1*-deficient MPNST cell lines. From the DS-10, *Bmp2* was chosen for further study based on (i) the significance in GSEA, and (ii) the positive association between *Bmp2* expression and increasing malignancy of NF1-related tissues in the data of Miller and colleagues (13). In addition, a case report suggested a connection between acute deterioration of plexiform neurofibroma to MPNST and BMP2 treatment intended to facilitate bone fusion after surgery (41).

Bmp2 overexpression resulting from *Nf1* deficiency but independent of NRAS and MEK1/2 activities was verified in MPNST cells by qPCR. Although a weak association of NRAS and SMAD signaling was observed, the effect of BMP2 on SMAD 1/5/8 signaling was far stronger than that of NRAS, indicating that BMP2-SMAD1/5/8 may contribute independently to MPNST formation or malignant phenotypes, via mechanisms to control cell migration, invasiveness, and tumor growth, as it does in other tumor types (32). Although BMP2 and BMP4 have certain pathway and functional redundancy (42), these 2 factors had different mechanisms of gene regulation in this study. We did not find decreased *Bmp4* expression after inhibition of *NRas* by siRNA in our dataset, but we did find that the expression of *Gdf6*, also known as *Bmp13*, significantly increased in ST88-14 cells (DS-4) but decreased in si*N-Ras*-treated sample (DS-2). GDF6 is believed to bind the same type I and II receptors as BMP2, which results in phosphorylation/activation of SMAD1/5/8 (43). This mechanism may explain the phosphorylation/activation of SMAD1/5/8 that we observed in the regulation of SMAD1/5/8 by the NRAS pathway. Inhibition of BMP2-SMAD1/5/8 signaling by BMP2 shRNA interference or the BMP-receptor kinase inhibitor, LDN-193189, impaired the

motility and invasiveness of MPNST cell lines *in vitro*. Gordon and colleagues reported BMP2 could increase MMP2 (type IV collagenase) expression in a pancreatic cancer cell line through the SMAD1-dependent mechanism (22). This mechanism seems to be active in the MPNST cells that we tested, as *Mmp2* expression in T265 cells was downregulated by 0.1 μmol/L LDN-193189 after 48 hours treatment in culture (Supplementary Fig. S9A). LDN-193189 has been shown to suppress the activity of AKT and influence the malignant phenotypes of cancer cells (44). We also observed slightly decreased phosphorylation of AKT resulting from the knockdown *Bmp2* by siRNA in T265 and ST88-14 cells (Supplementary Fig. S9B) and this signaling axis has been reported to impair the malignant properties of several different cancers (45, 46). These mechanisms could also explain the impaired migration and invasiveness of MPNST cells in this study.

Using comparative gene expression profiling, we identified the relationship between the neurofibromin deficiency and BMP2 overexpression in MPNST cell lines. It is possible that BMP2 promotes cancer progression through autocrine and/or paracrine mechanisms as found in other tumor types (20, 22, 23). This mechanism is consistent with the important role of the tumor microenvironment in MPNST tumorigenesis (7, 47). Inhibition of BMP2 expression by RNA interference and the downstream pathway by the specific inhibitor showed that BMP2-SMAD1/5/8 signaling influenced the migration and invasion of MPNSTs. Although direct inhibition of this pathway did not significantly decrease the cell proliferation, it provided an additional option to control the malignant properties (migration and invasion) of MPNST, and the possible synergistic effects when it is applied with other treatments could provide new approaches to improve the MPNST therapy.

On the basis of the gene lists from various treatments in this study, additional mechanisms supporting NF1-related phenotypes can be proposed. Embryonic lethality due to failure of heart development in the *Nf1* knockout mouse model (48) and likewise the increased risk for a variety of cardiovascular disorders have to be identified in NF1 patients (49). Although the expression of neurofibromin GAP-related domain rescues the embryonic heart defects in $Nf1^{-/-}$ mouse, its mechanism downstream RAS signaling is still not clear. *Adm* gene, which was positively regulated by increased NRAS activity (DS-5), encodes the protein adrenomedullin that functions as systemic vasodilator and natriuretic peptide. High *Adm* mRNA level has been associated with hypertension (50) and myocyte hypertrophy (51, 52). NF1 patients frequently experience hypertension (53, 54), and in the *Nf1* knockout mouse model, Xu and colleagues reported that cardiomyocyte-specific knockdown of *Nf1* contributed to the cardiac hypertrophy (55). In DS-5, *Adm* mRNA increased in ST88-14 but was downregulated by si*NRas*, and these alterations in gene expression could serve as the mechanistic basis for an NF1-related cardiovascular disease study. We observed *Edn1* mRNA to be highly expressed in ST88-14 (DS-6), and EDN1 has been reported to play an important role in heart development (56) and has been associated with cardiac hypertrophy in patient cohort studies (57). These findings shed light on neurofibromin–NRAS–ADM and neurofibromin–MEK1/2–EDN1 axes identified in MPNST cells in this study, and could expand our understanding of molecular mechanisms for cardiovascular diseases in NF1 patients.

In summary, we investigated differential gene expression in MPNST cell lines to identify novel functions of neurofibromin and potential drug targets for MPNST. In particular, we found that BMP2 signaling is an NRAS- and MEK1/2-independent effect of neurofibromin deficiency in the MPNSTs.

Disclosure of Potential Conflicts of Interest

No potential conflicts of interest were disclosed.

Authors' Contributions

Conception and design: D. Sun, M.A. Tainsky
Development of methodology: D. Sun, J.M. Kraniak, M.A. Tainsky
Acquisition of data (provided animals, acquired and managed patients, provided facilities, etc.): D. Sun, R. Haddad, S.D. Horne, M.A. Tainsky
Analysis and interpretation of data (e.g., statistical analysis, biostatistics, computational analysis): D. Sun, R. Haddad, M.A. Tainsky
Writing, review, and/or revision of the manuscript: D. Sun, M.A. Tainsky
Administrative, technical, or material support (i.e., reporting or organizing data, constructing databases): M.A. Tainsky
Study supervision: J.M. Kraniak, M.A. Tainsky

Acknowledgments

References

1. Mattingly RR, Kraniak JM, Dilworth JT, Mathieu P, Bealmear B, Nowak JE, et al. The mitogen-activated protein kinase/extracellular signal-regulated kinase kinase inhibitor PD184352 (CI-1040) selectively induces apoptosis in malignant schwannoma cell lines. J Pharmacol Exp Ther 2006;316:456–65.
2. Martin GA, Viskochil D, Bollag G, McCabe PC, Crosier WJ, Haubruck H, et al. The GAP-related domain of the neurofibromatosis type 1 gene product interacts with ras p21. Cell 1990;63:843–9.
3. Evans DG, Baser ME, McGaughran J, Sharif S, Howard E, Moran A. Malignant peripheral nerve sheath tumours in neurofibromatosis 1. J Med Genet 2002;39:311–4.
4. Sorensen SA, Mulvihill JJ, Nielsen A. Long-term follow-up of von Recklinghausen neurofibromatosis. Survival and malignant neoplasms. N Engl J Med 1986;314:1010–5.
5. Matsui I, Tanimura M, Kobayashi N, Sawada T, Nagahara N, Akatsuka J. Neurofibromatosis type 1 and childhood cancer. Cancer 1993;72:2746–54.
6. Le LQ, Liu C, Shipman T, Chen Z, Suter U, Parada LF. Susceptible stages in Schwann cells for NF1-associated plexiform neurofibroma development. Cancer Res 2011;71:4686–95.
7. Zhu Y, Ghosh P, Charnay P, Burns DK, Parada LF. Neurofibromas in NF1: Schwann cell origin and role of tumor environment. Science 2002;296:920–2.
8. Kalamarides M, Acosta MT, Babovic-Vuksanovic D, Carpen O, Cichowski K, Evans DG, et al. Neurofibromatosis 2011: a report of the Children's Tumor Foundation annual meeting. Acta Neuropathol 2012;123:369–80.
9. Dilworth JT, Wojtkowiak JW, Mathieu P, Tainsky MA, Reiners JJ Jr, Mattingly RR, et al. Suppression of proliferation of two independent NF1 malignant peripheral nerve sheath tumor cell lines by the pan-ErbB inhibitor CI-1033. Cancer Biol Ther 2008;7:1938–46.
10. Lee PR, Cohen JE, Tendi EA, Farrer R, GH DEV, Becker KG, et al. Transcriptional profiling in an MPNST-derived cell line and normal human Schwann cells. Neuron Glia Biol 2004;1:135–47.
11. Watson MA, Perry A, Tihan T, Prayson RA, Guha A, Bridge J, et al. Gene expression profiling reveals unique molecular subtypes of neurofibromatosis type I-associated and sporadic malignant peripheral nerve sheath tumors. Brain Pathol 2004;14:297–303.
12. Miller SJ, Rangwala F, Williams J, Ackerman P, Kong S, Jegga AG, et al. Large-scale molecular comparison of human schwann cells to malignant peripheral nerve sheath tumor cell lines and tissues. Cancer Res 2006;66:2584–91.
13. Miller SJ, Jessen WJ, Mehta T, Hardiman A, Sites E, Kaiser S, et al. Integrative genomic analyses of neurofibromatosis tumours identify SOX9 as a biomarker and survival gene. EMBO Mol Med 2009;1:236–48.
14. Reynolds JE, Fletcher JA, Lytle CH, Nie L, Morton CC, Diehl SR. Molecular characterization of a 17q11.2 translocation in a malignant schwannoma cell line. Hum Genet 1992;90:450–6.
15. DeClue JE, Papageorge AG, Fletcher JA, Diehl SR, Ratner N, Vass WC, et al. Abnormal regulation of mammalian p21ras contributes to malignant tumor growth in von Recklinghausen (type 1) neurofibromatosis. Cell 1992;69:265–73.
16. Barkan B, Starinsky S, Friedman E, Stein R, Kloog Y. The Ras inhibitor farnesylthiosalicylic acid as a potential therapy for neurofibromatosis type 1. Clin Cancer Res 2006;12:5533–42.

17. Dahlberg WK, Little JB, Fletcher JA, Suit HD, Okunieff P. Radiosensitivity *in vitro* of human soft tissue sarcoma cell lines and skin fibroblasts derived from the same patients. Int J Radiat Biol 1993;63:191–8.

18. Kraniak JM, Sun D, Mattingly RR, Reiners JJ Jr, Tainsky MA. The role of neurofibromin in N-Ras mediated AP-1 regulation in malignant peripheral nerve sheath tumors. Mol Cell Biochem 2010;344:267–76.

19. Liu C, Tian G, Tu Y, Fu J, Lan C, Wu N. Expression pattern and clinical prognostic relevance of bone morphogenetic protein-2 in human gliomas. Jpn J Clin Oncol 2009;39:625–31.

20. Rothhammer T, Poser I, Soncin F, Bataille F, Moser M, Bosserhoff AK. Bone morphogenic proteins are overexpressed in malignant melanoma and promote cell invasion and migration. Cancer Res 2005;65:448–56.

21. Arnold SF, Tims E, McGrath BE. Identification of bone morphogenetic proteins and their receptors in human breast cancer cell lines: importance of BMP2. Cytokine 1999;11:1031–7.

22. Gordon KJ, Kirkbride KC, How T, Blobe GC. Bone morphogenetic proteins induce pancreatic cancer cell invasiveness through a Smad1-dependent mechanism that involves matrix metalloproteinase-2. Carcinogenesis 2009;30:238–48.

23. Langenfeld EM, Calvano SE, Abou-Nukta F, Lowry SF, Amenta P, Langenfeld J. The mature bone morphogenetic protein-2 is aberrantly expressed in non–small cell lung carcinomas and stimulates tumor growth of A549 cells. Carcinogenesis 2003;24:1445–54.

24. Werner T. Bioinformatics applications for pathway analysis of microarray data. Curr Opin Biotechnol 2008;19:50–4.

25. Liang G, Bansal G, Xie Z, Druey KM. RGS16 inhibits breast cancer cell growth by mitigating phosphatidylinositol 3-kinase signaling. J Biol Chem 2009;284:21719–27.

26. Meloche S, Pouyssegur J. The ERK1/2 mitogen-activated protein kinase pathway as a master regulator of the G_1- to S-phase transition. Oncogene 2007;26:3227–39.

27. Stow LR, Jacobs ME, Wingo CS, Cain BD. Endothelin-1 gene regulation. FASEB J 2011;25:16–28.

28. Sunaga N, Shames DS, Girard L, Peyton M, Larsen JE, Imai H, et al. Knockdown of oncogenic KRAS in non–small cell lung cancers suppresses tumor growth and sensitizes tumor cells to targeted therapy. Mol Cancer Ther 2011;10:336–46.

29. St Hilaire C, Ziegler SG, Markello TC, Brusco A, Groden C, Gill F, et al. NT5E mutations and arterial calcifications. N Engl J Med 2011;364:432–42.

30. Edwards NL, Magilavy DB, Cassidy JT, Fox IH. Lymphocyte ecto-5′-nucleotidase deficiency in agammaglobulinemia. Science 1978;201:628–30.

31. Zhi X, Wang Y, Zhou X, Yu J, Jian R, Tang S, et al. RNAi-mediated CD73 suppression induces apoptosis and cell-cycle arrest in human breast cancer cells. Cancer Sci 2010;101:2561–9.

32. Singh A, Morris RJ. The Yin and Yang of bone morphogenetic proteins in cancer. Cytokine Growth Factor Rev 2010;21:299–313.

33. Massague J, Seoane J, Wotton D. Smad transcription factors. Genes Dev 2005;19:2783–810.

34. Barkan B, Kloog Y, Ehrlich M. Phenotypic reversion of invasive neurofibromin-deficient schwannoma by FTS: Ras inhibition reduces BMP4/Erk/Smad signaling. Mol Cancer Ther 2011;10:1317–26.

35. Wong WW, Hirose T, Scheithauer BW, Schild SE, Gunderson LL. Malignant peripheral nerve sheath tumor: analysis of treatment outcome. Int J Radiat Oncol Biol Phys 1998;42:351–60.

36. Clement JH, Raida M, Sanger J, Bicknell R, Liu J, Naumann A, et al. Bone morphogenetic protein 2 (BMP-2) induces *in vitro* invasion and *in vivo* hormone independent growth of breast carcinoma cells. Int J Oncol 2005;27:401–7.

37. Vogt J, Traynor R, Sapkota GP. The specificities of small molecule inhibitors of the TGFss and BMP pathways. Cell Signal 2011;23:1831–42.

38. Ismat FA, Xu J, Lu MM, Epstein JA. The neurofibromin GAP-related domain rescues endothelial but not neural crest development in Nf1 mice. J Clin Invest 2006;116:2378–84.

39. Ho IS, Hannan F, Guo HF, Hakker I, Zhong Y. Distinct functional domains of neurofibromatosis type 1 regulate immediate versus long-term memory formation. J Neurosci 2007;27:6852–7.

40. Widemann BC, Salzer WL, Arceci RJ, Blaney SM, Fox E, End D, et al. Phase I trial and pharmacokinetic study of the farnesyltransferase inhibitor tipifarnib in children with refractory solid tumors or neurofibromatosis type I and plexiform neurofibromas. J Clin Oncol 2006;24:507–16.

41. Steib JP, Bouchaib J, Walter A, Schuller S, Charles YP. Could an osteoinductor result in degeneration of a neurofibroma in NF1? Eur Spine J 2010;19(Suppl 2):S220–5.

42. Fritz DT, Liu D, Xu J, Jiang S, Rogers MB. Conservation of Bmp2 post-transcriptional regulatory mechanisms. J Biol Chem 2004;279:48950–8.

43. Williams LA, Bhargav D, Diwan AD. Unveiling the bmp13 enigma: redundant morphogen or crucial regulator? Int J Biol Sci 2008;4:318–29.

44. Hao J, Ho JN, Lewis JA, Karim KA, Daniels RN, Gentry PR, et al. *In vivo* structure–activity relationship study of dorsomorphin analogues identifies selective VEGF and BMP inhibitors. ACS Chem Biol 2010;5:245–53.

45. Kang MH, Kim JS, Seo JE, Oh SC, Yoo YA. BMP2 accelerates the motility and invasiveness of gastric cancer cells via activation of the phosphatidylinositol 3-kinase (PI3K)/Akt pathway. Exp Cell Res 2010;316:24–37.

46. Peart TM, Correa RJ, Valdes YR, Dimattia GE, Shepherd TG. BMP signalling controls the malignant potential of ascites-derived human epithelial ovarian cancer spheroids via AKT kinase activation. Clin Exp Metastasis 2012;29:293–313.

47. Yang FC, Ingram DA, Chen S, Zhu Y, Yuan J, Li X, et al. Nf1-dependent tumors require a microenvironment containing $Nf1^{+/-}$ and c-kit-dependent bone marrow. Cell 2008;135:437–48.

48. Brannan CI, Perkins AS, Vogel KS, Ratner N, Nordlund ML, Reid SW, et al. Targeted disruption of the neurofibromatosis type-1 gene leads to developmental abnormalities in heart and various neural crest-derived tissues. Genes Dev 1994;8:1019–29.

49. Friedman JM, Arbiser J, Epstein JA, Gutmann DH, Huot SJ, Lin AE, et al. Cardiovascular disease in neurofibromatosis 1: report of the NF1 Cardiovascular Task Force. Genet Med 2002;4:105–11.

50. Jiang W, Jiang HF, Pan CS, Cai DY, Qi YF, Pang YZ, et al. Relationship between the contents of adrenomedullin and distributions of neutral endopeptidase in blood and tissues of spontaneously hypertensive rats. Hypertens Res 2004;27:109–17.

51. Tsuruda T, Jougasaki M, Boerrigter G, Costello-Boerrigter LC, Cataliotti A, Lee SC, et al. Ventricular adrenomedullin is associated with myocyte hypertrophy in human transplanted heart. Regul Pept 2003;112:161–6.

52. Romppanen H, Marttila M, Magga J, Vuolteenaho O, Kinnunen P, Szokodi I, et al. Adrenomedullin gene expression in the rat heart is stimulated by acute pressure overload: blunted effect in experimental hypertension. Endocrinology 1997;138:2636–9.

53. Montani D, Coulet F, Girerd B, Eyries M, Bergot E, Mal H, et al. Pulmonary hypertension in patients with neurofibromatosis type I. Medicine 2011;90:201–11.

54. Demarchi I, Genoni G, Prodam F, Petri A, Busti A, Cortese L, et al. [Neurofibromatosis type 1 and hypertension in pediatrics: case report]. Minerva Pediatr 2011;63:335–9.

55. Xu J, Ismat FA, Wang T, Lu MM, Antonucci N, Epstein JA. Cardiomyocyte-specific loss of neurofibromin promotes cardiac hypertrophy and dysfunction. Circ Res 2009;105:304–11.

56. Chen M, Lin YQ, Xie SL, Wang JF. Mitogen-activated protein kinase in endothelin-1-induced cardiac differentiation of mouse embryonic stem cells. J Cell Biochem 2010;111:1619–28.

57. Castro MG, Rodriguez-Pascual F, Magan-Marchal N, Reguero JR, Alonso-Montes C, Moris C, et al. Screening of the endothelin1 gene (EDN1) in a cohort of patients with essential left ventricular hypertrophy. Ann Hum Genet 2007;71(Pt 5):601–10.